Neurochemistry International 126 (2019) 178–186

Contents lists available at ScienceDirect

Neurochemistry International

journal homepage: www.elsevier.com/locate/neuint

Poloxamer 188 rescues MPTP-induced lysosomal membrane integrity impairment in cellular and mouse models of Parkinson's disease

Hongli Dong[b,1], Yuanyuan Qin[c,1], Yuyu Huang[c], Dongliang Ji[a], Feng Wu[a,*]

[a] Department of Pharmacology, School of Pharmacy, Nantong University, 19 Qixiu Road, Nantong, 226001, Jiangsu, China
[b] Encephalopathy Department, Suzhou Hospital of Traditional Chinese Medicine (The Hospital in Suzhou Affiliated to Nanjing University of Chinese Medicine), 18 Yangsu Road, Suzhou, 215009, China
[c] Department of Pharmacy, Suzhou Hospital of Traditional Chinese Medicine (The Hospital in Suzhou Affiliated to Nanjing University of Chinese Medicine), 18 Yangsu Road, Suzhou, 215009, China

ARTICLE INFO

Keywords:
Poloxamer 188
Parkinson's disease
Ruptured lysosome
Autophagic flux impairment

ABSTRACT

Parkinson's disease (PD) is the second most common neurodegenerative disorder characterized by the progressive loss of dopaminergic (DA) neurons in the substantia nigra pars compacta (SNpc). Rupture of lysosome is a major cellular stress condition leading to cell death in PD. We have previously shown that environmental oxidative toxins could impair autophagic flux and lysosomal functions in PD. Poloxamer 188 (P188) is an amphipathic polymer which has cytoprotective effect in traumatic brain injury and stroke. But whether Dyrk1A could rescue lysosome malfunction-mediated DA neuron death and α-synuclein aggregation in PD is still unknown. In the present study, MPTP mice models and MPP^+-treated SH-SY5Y cells were used for study, and we found that P188 rescued MPP^+-induced lysosomal dysfunction and impaired autophagy flux in mild MPP^+-treated SH-SY5Y cells. P188 administration significantly restored lysosomal membrane integrity and prevented cathepsins leakage from the lysosomes into the cytoplasm, which triggered caspase-dependent apoptotic cell death in sub-acute MPTP mouse model and MPP^+-treated SH-SY5Y cells. Furthermore, P188 ameliorated α-synuclein accumulation and behavioral impairment in chronic MPTP mouse model with MPTP and probenecid treatment. P188 could alleviate MPTP-induced DA neurons damage by restoring lysosome function.

1. Introduction

Parkinson's disease (PD) is the second most common neurodegenerative disorder characterized by the motor symptoms of resting tremor, rigidity, and bradykinesia, which is due to the progressive loss of dopaminergic (DA) neurons in the substantia nigra pars compacta (SNpc). Lysosomes are the main degradative organelles, and the endocytic, phagocytic and autophagic vesicles ultimately move on microtubule tracks to fuse with them (Luzio et al., 2007). Lysosomes are responsible for the removal of long life proteins, such as aggregate-prone α-synuclein, and for the clearance of damaged organelles, such as mitochondria and lysosomes itself (Lazarou et al., 2015; Radulovic et al., 2018). DA neurons are especially vulnerable to α-synuclein oligomers, with its concomitant aggregation into inclusion bodies (Pujols et al., 2018), and to mitochondrial dysfunction (Burchell et al., 2013). Growing evidence suggests that lysosomal function impairment may contribute to the pathogenesis of PD. There are a decreased number of intraneuronal lysosomes, reduced levels of lysosomal-associated proteins, such as lysosomal-associated membrane protein 1 (LAMP1), LAMP2, and cathepsin D, and an increased number of undegraded autophagosomes in postmortem brain samples from PD patients (Chu et al., 2009; Dehay et al., 2010; Klaver et al., 2018). Mutations in lysosomal-related genes, such as glucocerebrosidase (*GBA*) and lysosomal type 5 P-type ATPase (*ATP13A2*), are involved in PD pathology (Alcalay et al., 2015; Wang et al., 2018). Besides genetic PD patients, plenty of evidence indicates that environmental oxidative toxins, such as rotenone, 1-methyl-4-phenyl-1, 2, 3, 6-tetrahydropyridine (MPTP) and paraquat, which could induce PD-like pathology in rodent models of PD, result in lysosomal membrane permeabilization (LMP)(Dehay et al., 2010; Fernandez et al., 2016; Wu et al., 2015). Only few compound, such as the mammalian target of rapamycin (mTOR)-independent autophagic inducer trehalose, could restore lysosomal function via TFEB activation to provide neuroprotection in various animal models of PD (He et al., 2016; Rusmini et al., 2018; Tanji et al., 2015). Although the

* Corresponding author. Department of Pharmacology, School of Pharmacy, Nantong University, Nantong, 226001, Jiangsu, China.
E-mail address: wf619@ntu.edu.cn (F. Wu).
[1] Hongli Dong and Yuanyuan Qin contributed equally to this study.

https://doi.org/10.1016/j.neuint.2019.03.013
Received 18 January 2019; Received in revised form 14 March 2019; Accepted 17 March 2019
Available online 20 March 2019
0197-0186/

mechanism underlying the neuroprotective effects of this drug remains elusive (Lee et al., 2018; Yoon et al., 2017), enhancement of lysosomal function seems to be a feasible neuroprotective strategy for PD.

Poloxamer 188 (P188) is a non-ionic surfactant, which has protective effect against membranes rupture induced by various types of injury, such as stroke, cortical spreading depression, traumatic brain injury, intracranial haemorrhage, and so on (Cadichon et al., 2007; Gu et al., 2013; Luo et al., 2013; Yildirim et al., 2015). P188 rescues all the diseases-induced cell death by restoring the membranes integrity. Since it could come across blood brain barrier (Singh-Joy and McLain, 2008), P188 has also been used as intranasal vehicle for delivery of rasagiline mesylate or selegiline in the treatment of PD (Ravi et al., 2015; Rukmangathen et al., 2018). P188 increases fetal DA cell survival and DA fibre density in the striatum after neural transplantation, due to the prevention of membrane disruption (Quinn et al., 2008). All of these show important implications that P188 might play a key role in inhibiting environmental toxins damage and rescuing LMP-mediated DA neuron death in PD.

2. Experimental procedures

2.1. Animal and treatment

Adult male C57BL/6 mice, weighing 25–30 g, were purchased from Slaccas (Shanghai, China). All the mice were housed and bred in accordance with the institutional guidelines for animal use and care, and the protocol was approved by the ethical committee of Nantong University. Mice were housed in a 12:12 h light/dark schedule and with ad libitum access to food and water. For sub-acute MPTP mouse model, animals were randomly divided into 4 groups, 16 mice in each group. MPTP (M0896, Sigma-Aldrich, St. Louis, MO) and P188 (Sigma-Aldrich) were dissolved in sterile saline. The model group was given MPTP 30 mg/kg intraperitoneally once a day for 5 consecutive days (Jackson-Lewis and Przedborski, 2007), and the therapeutic groups were injected with P188 (0.4 g/kg or 0.8 g/kg) 30 min after MPTP administration via tail vein in the first 5 days and twice a week in the next 21 days. Since the average number of apoptotic DA neurons in SNpc peaks at day 1 after MPTP administration (Tatton and Kish, 1997), 6 mice of each group were sacrificed at this day for apoptotic detection. The rest were sacrificed after 21 days. For chronic MPTP mouse model, animals were also randomly divided into 4 groups, 12 mice in each group. Model group mice received intraperitoneal injection of MPTP (25 mg/kg in saline) and probenecid (250 mg/kg in dimethyl sulfoxide, DMSO) twice a week (Ferguson et al., 2015). The same dosage of P188 was used for the therapeutic groups. Behavioral tests were assessed 5 weeks after MPTP plus probenecid treatment and then mice were sacrificed.

2.2. Plasmid and antibodies

The cDNA encoding mCherry-GFP-LC3 was inserted into the expression vector FUW from Addgene (Cambridge, MA, USA). The pH of the lumen of endosomes is between 5.5 and 6.1 and the PH value in lysosomes is about 4.7. GFP is acid-labile with a pKa of 6.0, while the pKa of red fluorescent mCherry is less than 4.5. Therefore, colocalization of both GFP and mCherry fluorescence indicates that an autophagosome has not fused with a lysosome or lysosome exhibits impaired function. In contrast, a mCherry signal without GFP corresponds to autophagolysosome. The polyclonal anti-P62 (P0067), anti-GAPDH (G9545) and monoclonal anti-GAPDH (SAB2100894), anti-β-actin (A5441), anti-tyrosine hydroxylase (TH), and anti-cathepsin B (C6243) were bought from Sigma (St. Louis, MO, USA). The polyclonal anti-TH (ab112), anti-microtubule-associated protein 1 light chain 3 (LC3) A/B (ab62721), anti-cathepsin L (ab58991) and anti-LAMP1 (ab24170) was from Abcam (Cambridge, MA, USA). The polyclonal α-synuclein (4179), anti-caspase-3 (9665) and anti-cleaved caspase-3 (9664) was from Cell Signaling Technology (Danvers, Massachusetts, USA). The monoclonal anti-Galectin-3 were from Santa Cruz Biotechnology (Santa Cruz, CA, USA). Fluorescent secondary antibodies (anti-mouse 926–32212, anti-rabbit 926–32213) were from LI-COR Biosciences (Lincoln, Nebraska, USA).

2.3. Cell culture and transfection

Human neuroblastoma (SH-SY5Y) cells were maintained in Dulbecco's modified Eagle's medium (DMEM-F12) supplemented with 10% fetal bovine serum (Invitrogen, Carlsbad, CA, USA) at 37 °C in a humidified atmosphere of 5% CO_2 and 95% air. All transfections were performed in triplicate with Lipofectamine 2000 (Invitrogen) according to the manufacturer's manual. After the cell density reached about 80% in plastic flasks, SH-SY5Y cells were trypsinizated and transferred to 96-well plates for cell viability assay, 12-well plates for immunoblotting, and 24-well plates for immunofluorescence. The cells were pretreated with P188 10^{-6}-10^{-3} M (P2164009, Sigma-Aldrich, St. Louis, MO, USA) for 1 h before 1-methyl-4-phenylpyridinium (MPP^+, D048, Sigma-Aldrich, St. Louis, MO, USA) 100 μM treatment. SH-SY5Y cells were pretreated with CA-074 methyl ester (C5857, Sigma-Aldrich, St. Louis, MO, USA) or E64 (E3132, Sigma-Aldrich, St. Louis, MO, USA) for 30 min. Bafilomycin A1 (10 nM, 196000, Sigma-Aldrich, St. Louis, MO, USA) was added 30 min before cell harvest. Cell viability after MPP^+ 100 μM treatment for 48 h was estimated with cell counting kit-8 (CCK8, Dojindo, Kumamoto, Japan).

2.4. Immunohistochemistry and immunofluorescence

After P188 treatment for 21 days, mice were anesthetized with 4% sodium pentobarbital and then perfused with ice-cooled 0.01 M phosphate-buffered saline (PBS) and 4% paraformaldehyde sequentially. Then the whole brains were fixed in 4% paraformaldehyde for 6 h and dehydrated with sucrose solutions for 2 days. Midbrain (from approximately −2.5 to −3.88 mm relative to bregma, according to the whole mouse brain atlas) and striatum (approximately +1.2, 1.08, 0.96, 0.84 and 0.72 mm relative to bregma) sections were prepared at 40 μm with a freezing microtome (CM1900, Leica, Heidelberger, Nussloch, Germany). For immunohistochemistry analysis, coronal sections were permeabilized with 0.5% Triton X-100 in PBS for 30 min, blocked with 5% horse serum for 1 h at room temperature, and then incubated with anti-TH antibody overnight at 4 °C followed by incubation with biotin-conjugated anti-mouse antibody (Vector Labs, Burlingame, CA, USA). The avidin–biotin complex (ABC) Elite kit (Vector Labs, Burlingame, CA, USA) and 3, 3′-diaminobenzidine tetrachloride (DAB, Sigma-Aldrich) were used to visualize the final product. The stereological analyse was performed under the 200 × magnification of an Olympus B × 52 microscope (Olympus America Inc, Melville, NY) and stereologic assessment of TH-positive cell number was counted using Stereo Investigator 7 (MBF bioscience, Williston, VT). Estimated numbers of TH-positive cells were calculated from the numbers of counted neurons and the corresponding sampling probability. The outlined frame size in SNpc was 50 × 50 μm and the sampling grid size was 100 × 100 μm. A coefficient error of less than 0.10 was accepted. Each brain contains 10 consecutive sections at a three intervals and the number of DA neurons in the SNpc was counted from five mouse brains per group. The stereology was blinded to all treatment groups for each experiment. TH-positive optical density of striatum was measured with 5 coronal sections each animal from 5 mouse brains per group using the ImageJ software (v1.47, National Institutes of Health, USA). The measured values were corrected by subtracting value of nonspecific background obtained from the cortex. The data are expressed as a percentage of the corresponding area from the intact side. Immunoreactivity in double-labeled sections was labeled using primary antibodies anti-TH, anti-Galectin-3 or anti-cleaved caspase-3 and appropriate fluorescent secondary antibodies (Boster, WuHan, Hubei, China). SH-SY5Y

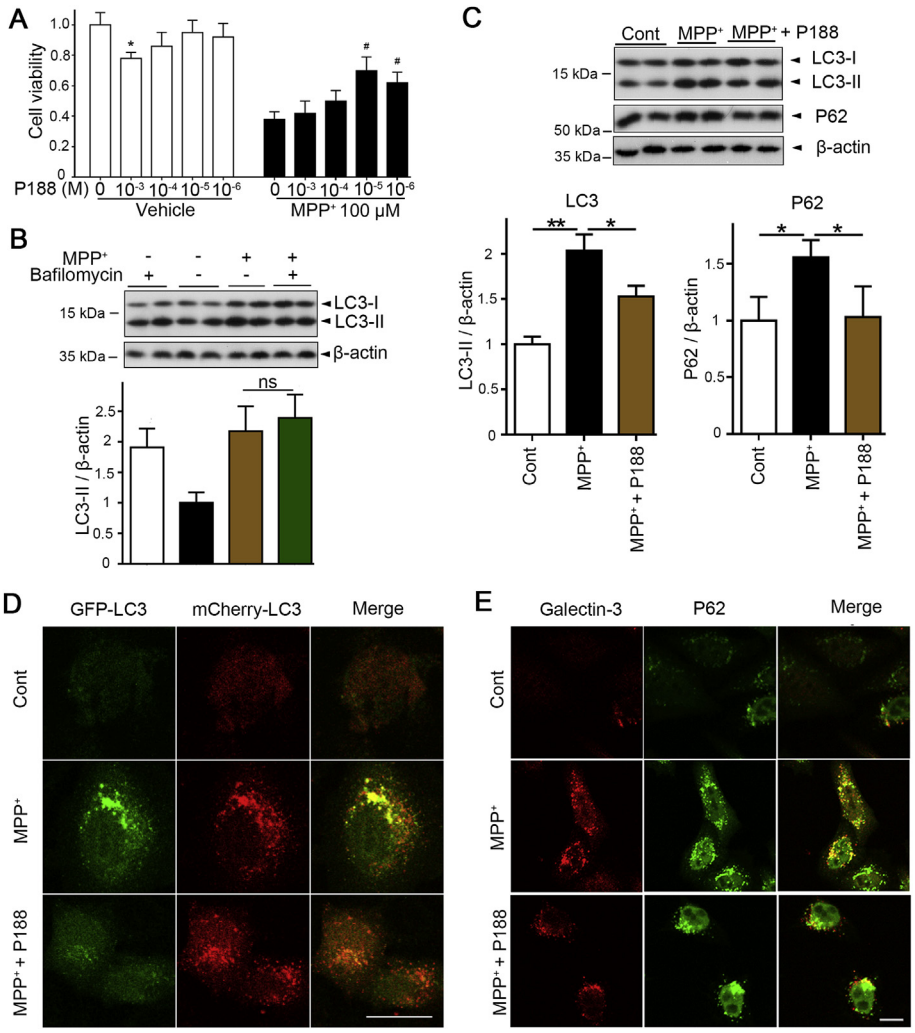

Fig. 1. P188 rescues MPP^+-induced lysosomal dysfunction and impaired autophagy flux in SH-SY5Y cells. (A) SH-SY5Y cells were treated with 10^{-6}-10^{-3} M P188 for 24 h or 100 μM MPP^+ plus P188 for 48 h. Cell viability was assessed using CCK8 kit. Cell survival was given as percent of control. Statistical significance was determined by a one-way ANOVA followed by the Newman-Keuls post hoc test. Data are expressed as mean ± SD (n = 3); *, $p < 0.05$ *vs.* without P188 group; #, $p < 0.05$ *vs.* without MPP^+ group. (B) SH-SY5Y cells were treated with 100 μM MPP^+ for 48 h. Bafilomycin A1 (10 nM) was added 30 min before cell harvest. Autophagic flux was calculated by dividing the level of LC3-II in the presence of bafilomycin A1 by that without bafilomycin A1. Statistical significance was determined by a one-way ANOVA followed by the Newman-Keuls post hoc test. Data are expressed as mean ± SD (n = 4). (C) SH-SY5Y cells were treated with 100 μM MPP^+ for 48 h to induce lysosome damage. P188 was added 30 min before MPP^+ treatment. At the indicated time, cells treated with MPP^+ upregulated the proteins levels of LC3-II and p62. Statistical significance was determined by a one-way ANOVA followed by the Newman-Keuls post hoc test. Data are expressed as mean ± SD (n = 4); *, $p < 0.05$; **, $p < 0.01$ *vs.* MPP^+ group. (D) mCherry-GFP-LC3 was transferred into SH-SY5Y cells for 24 h, and MPP^+ treatment increased the autophagic puncta (yellow puncta), and decreased the autophagolysosome puncta (red puncta) which was alleviated by P188 treatment for the next 48 h. (E) SH-SY5Y cells were fixed 1 h after washout, and were stained with P62 and Galectin-3 antibodies, and analyzed by confocal microscopy. P188 treatment reduced MPP^+-induced cytosolic Galectin-3-positive puncta and colocalization with recruited P62 which indicated initiation of autophagy of the damaged lysosomes. Scale bar = 20 μm.

cells, cultured on Poly-L-Lysine coated glass coverslips, were fixed in 4% paraformaldehyde for 20 min and then permeabilized with 0.15% Triton X-100 for 10 min, followed by blocking with 5% horse serum for 1 h. Cells were incubated with anti-P62 and anti-Galectin-3 and appropriate fluorescent secondary antibodies. Images were captured with a laser-scanning confocal unit (Zeiss LSM 710, Carl Zeiss, Jena, Germany).

2.5. Biogenic amine concentrations analysis

After the sacrifice of the mice, dissected striatum was weighted rapidly and then sonicated in ice-cooled 0.4 mol/L perchloric acid with 0.01% EDTA (1:10, w/v). Concentrations of DA and its main metabolites, 3,4-dihydroxyphenylacetic acid (DOPAC) and homovanillic acid (HVA) were measured with high-performance liquid chromatography with electrochemical detection (HPLC-ECD). Samples were centrifuged at 15,000 g for 30 min and the supernatant was collected through a 0.22 μm filter membrane. Sample (10 μl) was injected using a Waters 717 Autosampler (Waters, Milford, MA, USA) connected to a Waters 1525 HPLC pump. The sample was passed over an Atlantis C 18 column. Analytes were detected using the Waters 2465 electrochemical detector (potential 600 mV). The mobile phase consisted of 50 mM sodium dihydrogenphosphate, 0.25 mM 1-octanesulfonic acid, 50 mM sodium citrate, 2 mM NaCl, 20 mg ethylendiaminetetraacetic acid disodium and acetonitrile (1:3, v/v). All components were adjusted to pH 4.3 with phosphoric acid, pumped at a flow rate of 1 ml/min. Quantitation was achieved by the use of each standard curve. Data were normalized to brain tissue weight.

2.6. Western blot analysis

Mouse ventral midbrain homogenates and SH-SY5Y cells were lysed in 1 × Laemmli sample buffer (125 mM Tris-HCl, pH 6.8, 2% SDS, 10% glycerol, 10% 2-mercaptoethanol, and 0.01% bromphenol blue) and boiled for 10 min. Protein concentration was determined with BCA protein assay kit (T9300A, Takara Bio, Shiga, Japan). Equal amounts of protein were separated by sodium dodecyl sulfate (SDS)-polyacrylamide gel electrophoresis (PAGE) and transferred onto NC membranes, respectively. Membranes were blocked with 5% fat-free milk in TBST (50 mM Tris-HCl, pH 7.4, 150 mM NaCl, 0.05% Tween 20) for 30 min at room temperature and then incubated overnight with primary antibody diluted in 5% skimmed milk in TBST. After washing with TBST, membranes were incubated with appropriate fluorescent secondary antibodies for 2 h at room temperature. The signal was detected with Odyssey Two-Color Infrared Imaging System (LI-COR, Linclon, Nebraska, USA). Densitometry was quantified by ImageJ software.

2.7. Subcellular fractionation purification and lysosomal-leakiness assay

Harvested SH-SY5Y cells were homogenized in subcellular fractionation buffer by tissue grinder with lysosome enrichment kit for tissue and cultured cells (Pierce Biotechnology, Rockford, USA). Centrifuged at 500 *g* for 10 min at 4 °C, the supernatant was spun at 145,000 *g* in OptiPrep gradients media for 2 h at 4 °C with Beckman Coulter

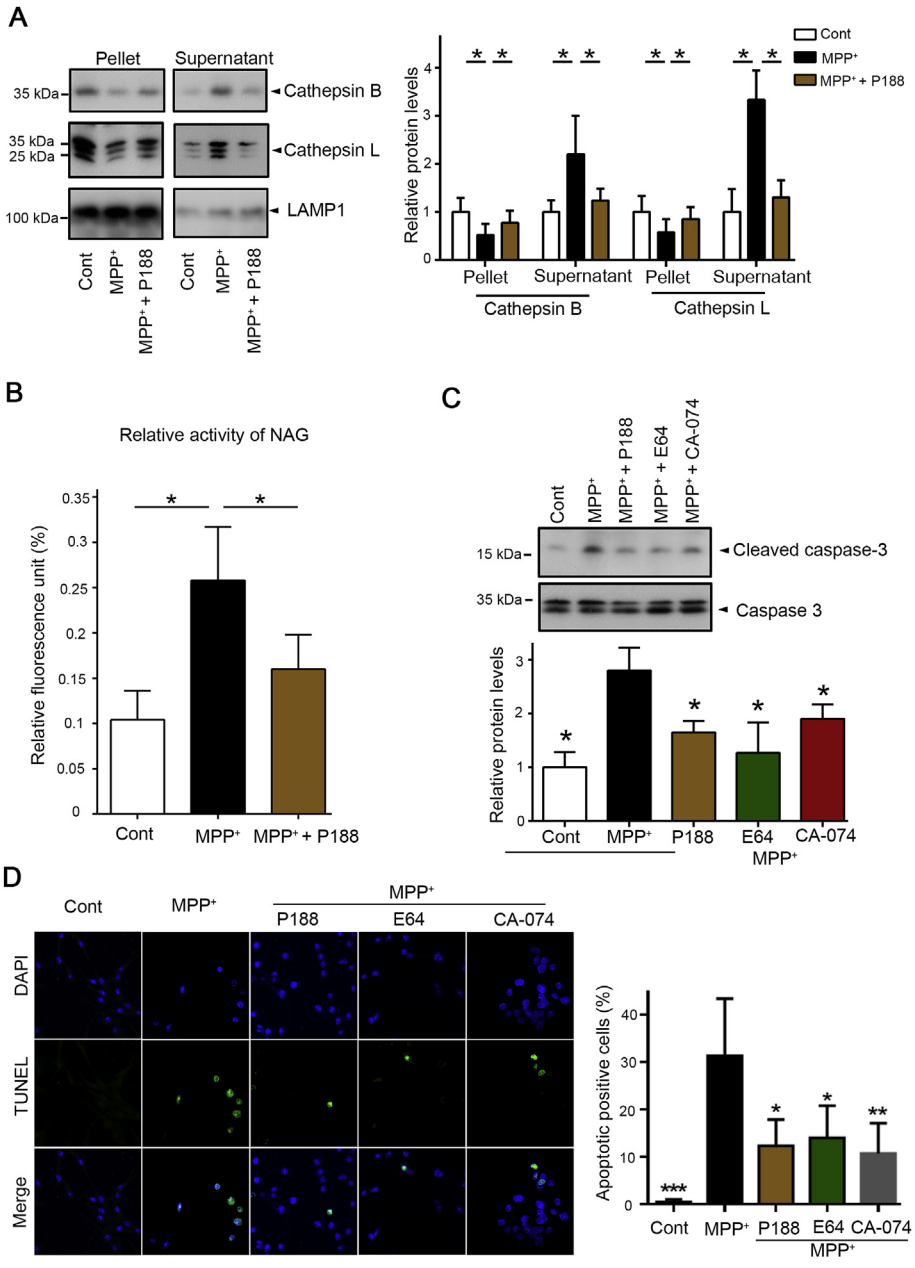

Fig. 2. P188 reduces LMP-mediated cell apoptosis in SH-SY5Y cells. (A) SH-SY5Y cells were treated with vehicle or 100 μM MPP^+ for 48 h. P188 was added 30 min before MPP^+ treatment. After the lysosomal fraction was incubated for 60 min at 37 °C with gentle agitation, MPP^+ caused a greater loss of cathepsin B/L from lysosomes, and P188 could alleviate cathepsins leakage. Statistical significance was determined by a one-way ANOVA followed by the Newman-Keuls post hoc test. Data are expressed as mean ± SD (n = 3); *, $p < 0.05$. (B) Activity of released NAG from lysosome had also shown that LMP occurred in MPP^+-treated SH-SY5Y cells and P188 could maintain the lysosomal membrane integrity. Statistical significance was determined by a one-way ANOVA followed by the Newman-Keuls post hoc test. Data are expressed as mean ± SD (n = 3); *, $p < 0.05$. (C) Before treatment with MPP^+ for 48 h, P188, E64, and CA-074 were added to the culture media, caspase-3 and cleaved caspase-3 levels were analyzed by immunoblotting. Statistical significance was determined by a one-way ANOVA followed by the Newman-Keuls post hoc test. Data are expressed as mean ± SD (n = 3); *, $p < 0.05$ *vs.* MPP^+ group. (D) Apoptosis of SH-SY5Y cells were detected in TUNEL staining after MPP^+ exposure with or without P188, E64, or CA-074 pretreatment. Scale bar = 20 μm. Statistical significance was determined by a one-way ANOVA followed by the Newman-Keuls post hoc test. Data are expressed as mean ± SD (n = 4); *, $p < 0.05$; **, $p < 0.01$; ***, $p < 0.001$ *vs.* MPP^+ group.

OptimaTM L-90K Ultracentrifuge (Fullerton, CA, USA). The lysosome fraction was purified from OptiPrep media and then incubated for 60 min at 37 °C. Finally, this subcellular fractionation was re-pelleted at 13,800 *g* for 15 min at 4 °C, and the pellet and supernatant were analyzed with Western blot analysis.

2.8. Lysosomal integrity detection

Assessing lysosomal integrity, activity of released N-acetyl-beta-D-glucosaminidase (NAG) was measured with NAG release test Kit (GENMED, Shanghai, China). 4-Methylumbelliferyl-β-D-glucoside (MUG) was a specific fluorogenic substrate of NAG. The excitation and emission wavelength was 365 nm and 444 nm, and the level of actual sample relative fluorescence unit (RFU) was normalized to total sample RFU.

2.9. TUNEL staining

SH-SY5Y cells were seeded onto 24-well plates and pretreated with 10 μM P188 or cathepsins inhibitors including CA-074 (50 μM) or E64 (10 μg/ml) for 30 min, then exposed to 100 μM MPP^+ for 48 h. Apoptotic cells were identified with DAPI nuclear stain and terminal deoxynucleotidyl transferase-mediated dUTP-biotin nick end labeling (TUNEL) assay using the One Step Tunel Apoptosis Assay kit (Beyotime, Haimen, Jiangsu, China) following the manufacture's instructions. The cells were observed using fluorescence microscopy (Nikon TE2000U, Tokyo, Japan) and both the TUNEL positive cells and DAPI stained nuclei were counted in three independent experiments.

2.10. Behavioral analysis

Chronic MPTP mouse model exhibits behavioral deficits (Ferguson et al., 2015), and the neuroprotective effect of P188 was evaluated by grip strength and pole tests. Mice were divided into 4 groups, 12 mice in each group, such as vehicle group, MPTP group, P188 L (0.4 g/kg) group, and P188 H (0.8 g/kg) group. All tests were performed during the light cycle by an experimenter blind to treatment group. *Grip strength*. Mice were allowed to grasp a metal grid either with their fore-

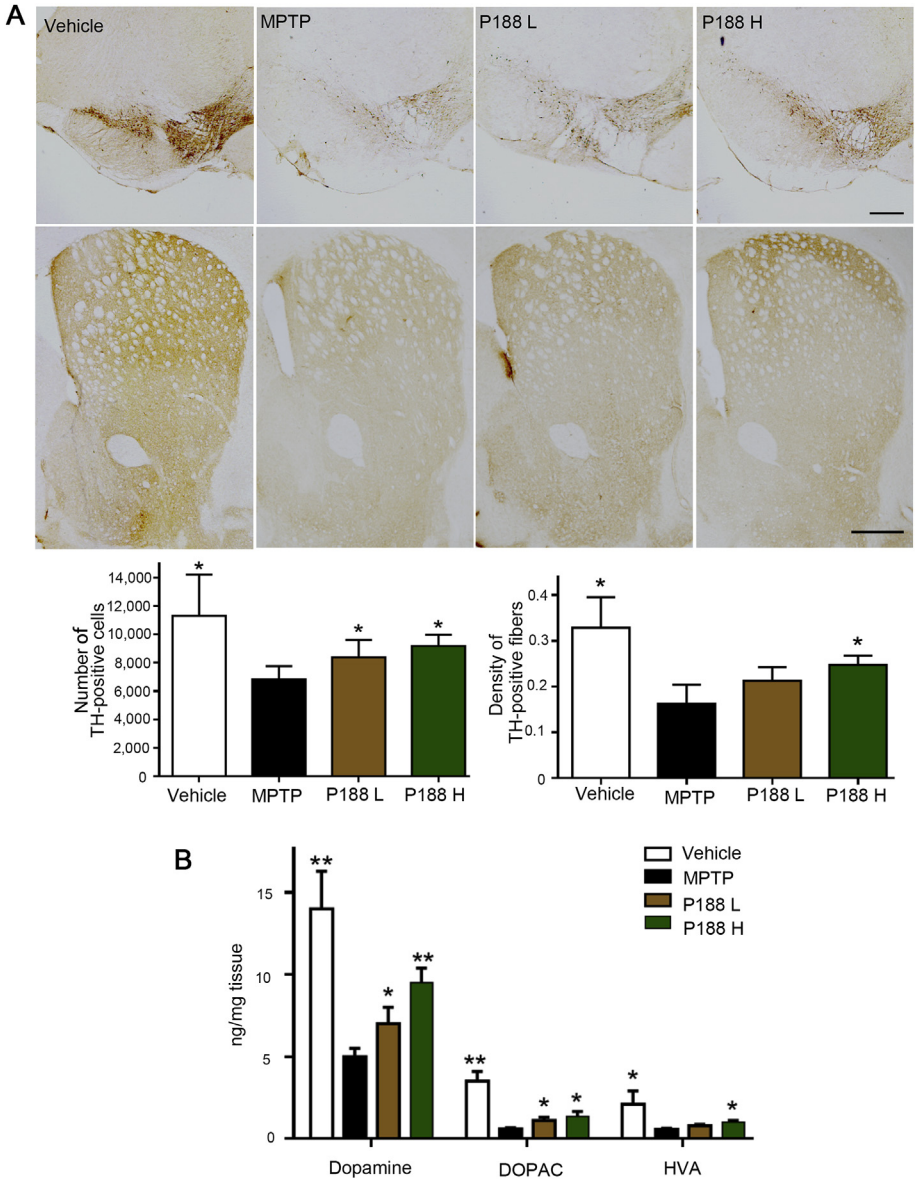

Fig. 3. P188 alleviates DA neurons damage in SNpc of sub-acute MPTP mouse model. (A) After P188 treatment for 21 days, mice were sacrificed and brain sections from striatum and SNpc were subjected to immunostaining with anti-TH antibody. P188 preserved DA neurons in SNpc of MPTP-treated mice. Scale bar = 2 mm. Statistical significance was determined by a one-way ANOVA followed by the Newman-Keuls post hoc test. Data are expressed as mean ± SD (n = 5); *, $p < 0.05$ *vs.* MPTP group. (B) DA, DOPAC and HVA concentrations in the striatum of MPTP-injected mice with P188 or not, were measured 21 days after MPTP treatment with HPLC-ECD. Statistical significance was determined by a one-way ANOVA followed by the Newman-Keuls post hoc test. Data are expressed as mean ± SD (n = 10); *, $p < 0.05$; **, $p < 0.01$ *vs.* MPTP group.

limbs or both of fore- and hind-limbs. Mouse tail was holded and the force transducer was used to measure kilogram of the maximum holding force when the mouse released their grasp on the grid. *Pole test.* The pole was wrapped with bandage gauze. First, all mice received three training trials per day for two consecutive days. On the third day, mouse was placed on the top of the pole facing head-up. The time taken to turn and total time taken to reach the base of the pole was recorded. The total time was no more than 2 min.

2.11. Statistical analysis

Data were presented as mean ± SD. Results were compared by one-way ANOVA, with a threshold of $P < 0.05$, following post hoc analysis where appropriate. Statistical comparisons were performed using GraphPad Prism 6.0 Software (GraphPad Software Inc., San Diego, CA, USA) and SPSS software (IBM SPSS Statistics 22, Chicago, IL, USA).

3. Results

3.1. P188 rescues MPP^+-induced lysosomal dysfunction and impaired autophagy flux in SH-SY5Y cells

P188 itself resulted in cell toxicity at high concentration, while P188 at low concentration, such as 10^{-6} M and 10^{-5} M, could obviously alleviate MPP^+-induced SH-SY5Y cells damage (Fig. 1, A). Therefore, the final concentration of P188 for treatment was 10 μM. Mild MPP^+ exposure impaired autophagosome degradation (Miyara et al., 2016; Sakamoto et al., 2017), and 100 μM MPP^+ was chosen to investigate the effect of MPP^+ at low dosage on autophagic processes. Autophagic flux was measured by the conversion of LC3-I to LC3-II. Bafilomycin A1 is a macrolide antibiotic which could inhibit vacuolar-type ATPase to disrupt vesicular acidification. It did not further increase the level of LC3-II compared with MPP^+ treatment group, indicating that the increased LC3-II was due to the stalling of autophagy (Fig. 1, B). We observed that besides upregulation of LC3-II, autophagic substrate P62 was also significantly increased with MPP^+ treatment. P188 could decrease both of the protein levels (Fig. 1, C). Meanwhile, SH-SY5Y cells were transfected with mCherry-GFP-tagged LC3 to monitor autophagic flux, and GFP signal was quenched quickly in the

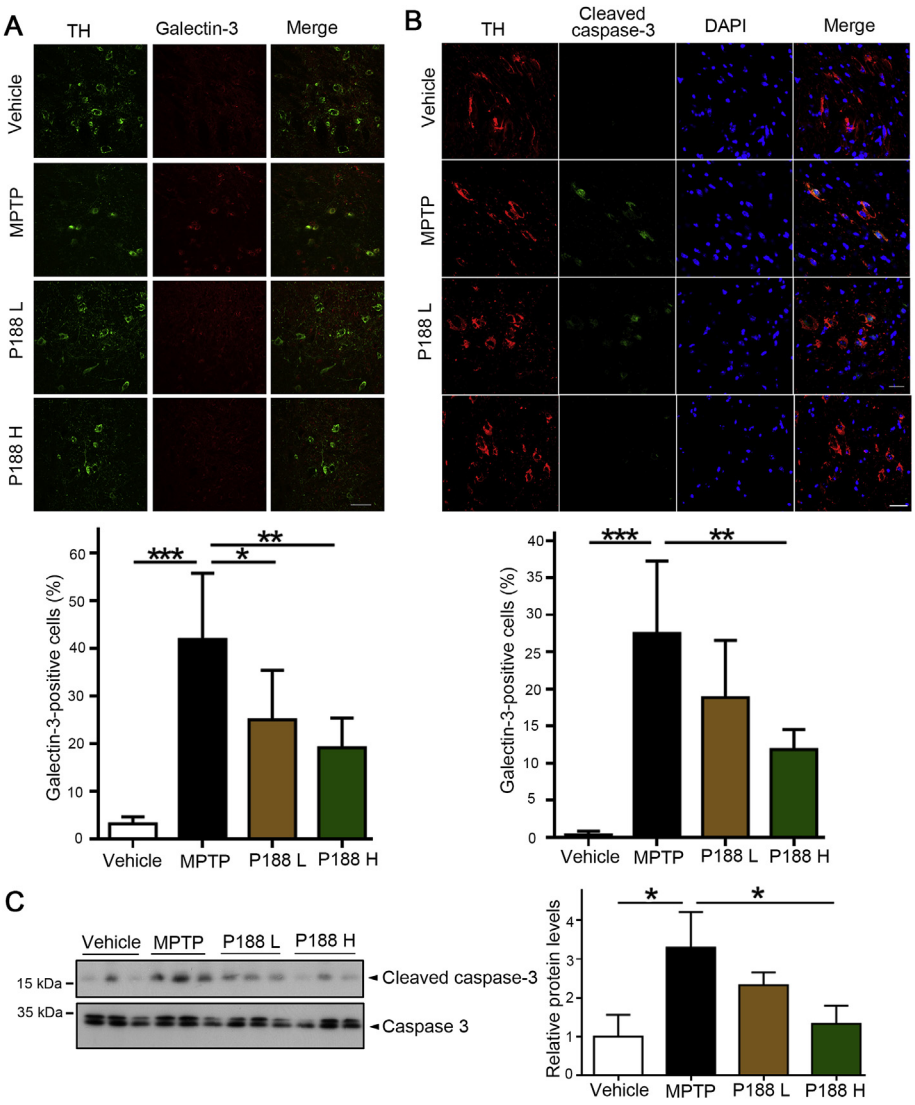

Fig. 4. P188 ameliorates lysosomal malfunction in sub-acute MPTP mouse model. (A) 21 days after MPTP or vehicle injection with P188 or not, ventral midbrain was immunostained for Galectin-3 and TH. The Galectin-3-positive DA neurons were increased in MPTP-treated mice, while P188 could reduce the lysosome damage. Scale bar = 20 μm. Statistical significance was determined by a one-way ANOVA followed by the Newman-Keuls post hoc test. Data are expressed as mean ± SD (n = 5); *, $p < 0.05$; **, $p < 0.01$; ***, $p < 0.001$ *vs.* MPTP group. (B) The ventral midbrain sections was immunostained for cleaved caspase-3 and TH. The apoptotic DA neurons were increased in MPTP-treated mice, while P188 could reduce cell death. Scale bar = 20 μm. Statistical significance was determined by a one-way ANOVA followed by the Newman-Keuls post hoc test. Data are expressed as mean ± SD (n = 5); **, $p < 0.01$; ***, $p < 0.001$ *vs.* MPTP group. (C) The ventral midbrain tissues were dissected, and caspase-3 and cleaved caspase-3 levels were analyzed by immunoblotting. Statistical significance was determined by a one-way ANOVA followed by the Newman-Keuls post hoc test. Data are expressed as mean ± SD (n = 6); *, $p < 0.05$ *vs.* MPTP group.

proteolytic conditions of the lysosome while mCherry was much more stable. MPP^+ treatment promoted autophagosome accumulation identified by the autophagic puncta (yellow puncta), and decreased the autophagolysosome puncta (red puncta), exhibiting autophagic flux impairment which was alleviated by P188 treatment (Fig. 1, D). To explore whether lysosomal damage was involved in the impaired autophagic flux, the translocation of cytosolic Galectin-3 was visualized, which was recruited to the lysosome membrane under various conditions that cause lysosome injury (Papadopoulos et al., 2017). The Galectin-3 staining showed a diffused pattern with few puncta in normal condition while Galectin-3-positive puncta were dramatically increased in MPP^+-treated group, and P188 treatment could reduced them (Fig. 1, E). Recruitment of P62 indicated initiation of autophagy of the damaged lysosomes (lysophagy), and we also found increased P62 co-localized with Galectin-3 with MPP^+ treatment, and with the treatment of P188 this co-localization dropped sharply (Fig. 1, E). These results confirm that P188 restores lysosomal integrity *in vitro*.

3.2. P188 reduces LMP-mediated cell apoptosis in SH-SY5Y cells

The membrane integrity of lysosomes from SH-SY5Y cells was measured by purified lysosomes incubation *in vitro*. MPP^+ treatment promoted cathepsins leakage from lysosomes, and P188 could retain cathepsins inside purified lysosomes (Fig. 2, A). The release of lysosomal enzyme NAG from lysosomes to cytoplasma was also increased in MPP^+-treated SH-SY5Y cells, and P188 significantly reduced the NAG release (Fig. 2, B). MPP^+ treatment dramatically upregulated the protein level of cleaved caspase-3. E64 is a membrane permeable cysteine protease inhibitor binding to an active thiol group in many cysteine proteases, such as cathepsins B, H, and L. CA-074 is an inhibitor of cathepsin B. Cathepsins leakage triggers cell apoptosis. Besides cathepsin inhibitors, P188 blunted MPP^+-induced upregulation of the cleaved caspase-3 in SH-SY5Y cells (Fig. 2, C). Meanwhile, P188 prevented MPP^+-induced SH-SY5Y cells apoptosis in TUNEL staining (Fig. 2, D). These results present that P188 treatment blunts MPP^+-induced LMP and alleviates cell apoptosis *in vitro*.

3.3. P188 alleviates DA neurons damage in SNpc through ameliorated lysosomal malfunction in sub-acute MPTP mouse model

Administration of P188 significantly preserved DA neurons in SNpc of MPTP-treated mice (Fig. 3, A). MPTP resulted in a significant reduction in DA and its metabolites, DOPAC and HVA. P188 treatment at low dosage (0.4 g/kg) increased the levels of DA and DOPAC while high dosage (0.8 g/kg) of P188 upregulated the levels of DA, DOPAC and HVA in mice striatum (Fig. 3, B). The number of Galectin-3 puncta in DA neurons was dramatically increased in MPTP-treated mice, while P188 could reduce the lysosome damage (Fig. 4, A). Immunoblot and

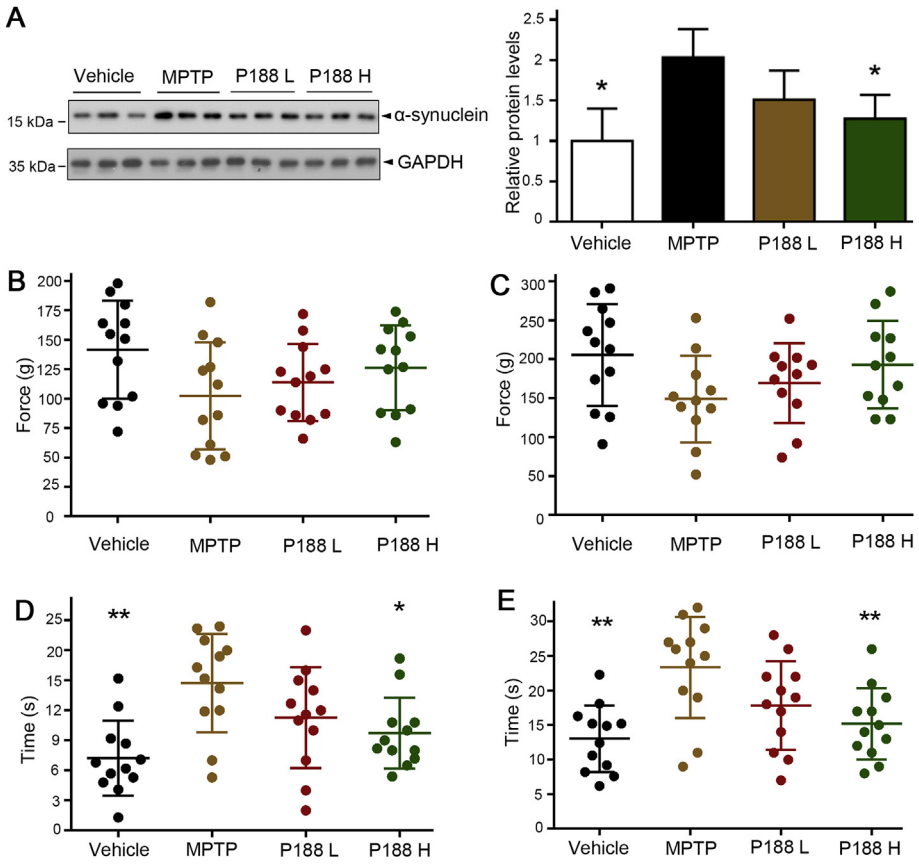

Fig. 5. P188 blunts α-synuclein accumulation and behavioral impairment in chronic MPTP mouse model. (A) 5 weeks after MPTP plus probenecid injection with P188 or not, the ventral midbrain tissues were dissected, and α-synuclein level was analyzed by immunoblotting. Statistical significance was determined by a one-way ANOVA followed by the Newman-Keuls post hoc test. Data are expressed as mean ± SD (n = 6); *, $p < 0.05$ *vs.* MPTP group. (B–E) At the indicated time, the grip strength of forelimb and forelimb plus hindlimb, and pole test of time to turn and time to reach the base were performed in the 4 groups. Behavioral abnormalities in the grip strength and pole test induced by MPTP were ameliorated with P188 treatment. Statistical significance was determined by a one-way ANOVA followed by the Newman-Keuls post hoc test. Data are expressed as mean ± SD (n = 12); *, $p < 0.05$; **, $p < 0.01$ *vs.* MPTP group.

immunofluorescence analysis demonstrated a significant upregulation in cleaved caspase-3 in MPTP mice and a sparing of the upregulation in P188 treatment (Fig. 4B and C). These results present that P188 treatment blunts LMP-induced DA neuron death in SNpc of sub-acute MPTP mouse model.

3.4. P188 ameliorates α-synuclein accumulation and behavioral impairment in chronic MPTP mouse model

Rodent model of PD with chronical MPTP and probenecid treatment exhibits granular and filamentous inclusions in DA neurons after 24 weeks (Meredith et al., 2002). Unfortunately, we didn't find any α-synuclein-positive inclusion in DA neurons 5 weeks after MPTP and probenecid treatment. However, Western blot analysis demonstrated a increase in α-synuclein accumulation in DA neurons and a sparing of the increase in P188 treatment (Fig. 5, A). Chronic MPTP mice exhibited significant impairment in the grip strength analysis because of reduced forelimb plus hindlimb strength. Although there was no statistic difference between therapeutic and model groups, P188 treatment group did show a trend of toward increasing grip strength (Fig. 5B and C). Pole test is also a sensitive behavioral indicator of dopaminergic function (Karuppagounder et al., 2014), and MPTP-treated mice showed increased time to turn, and increased time to reach the base while P188 treatment at high dosage could dramatically reduce the time compared with model group (Fig. 5D and E). These results suggest that P188 treatment reduce α-synuclein accumulation and ameliorate behavioral impairment in chronic MPTP mouse model.

4. Discussion

In the present study, we demonstrate for the first time that P188 rescues DA neurons damage which is due to neurotoxin-induced lysosomal dysfunction, and ameliorates α-synuclein accumulation and behavioral impairment in sub-acute and chronic rodent models of PD. Damaged lysosomes represent a potential hazard to DA neurons, because lysosomal dysfunction contributes to autophagic flux inhibition and facilitates intracellular protein accumulation, such as α-synuclein pathology, with their concomitant aggregation into inclusion bodies and subsequent DA neurons death (Wan et al., 2017). Therefore, lysosomal malfunction is a therapeutic target in PD, and P188 exerts the protective effects against pathological process mediated by neurotoxin MPTP.

Autophagy-lysosome pathway is involved in the protein quality control systems to maintain intracellular proteostasis. As one of PD hallmarks, intracellular inclusions in DA neurons of SNpc, known as Lewy bodies, is attributed to autophagic flux suppression. It has been reported that both the protein levels of LC3-II and p62 have been upregulated in Lewy bodies of postmortem brain samples from PD patients (Tanji et al., 2011; Zatloukal et al., 2002). MPTP is the only known dopaminergic neurotoxin resulting in a clinical syndrome in both humans and monkeys, and MPP^+ is its active toxic compound which is assimilated by DA neurons and inhibits complex I of the mitochondrial ETC (Jackson-Lewis and Przedborski, 2007). It has been reported that MPP^+ (10–200 μM) impairs autophagosome degradation (Miyara et al., 2016) and chronic MPTP mouse model exhibits slow progression of PD and formation of inclusion bodies (Meredith et al., 2002). To mimics the autophagic flux impairment pathology of PD, MPTP mice models and MPP^+-treated cell model were used to study the pharmacological effect of P188 in PD.

Autophagic flux impairment is due to suppressed autophagosome-lysosome fusion and lysosome malfunction. There are a decreased number of intraneuronal lysosomes and reduced cathepsins in postmortem brain samples from PD patients (Chu et al., 2009; Dehay et al., 2010; Klaver et al., 2018). Numerous endogenous and exogenous factors including reactive oxygen species (ROS), calpains, Ca^{2+}, TNFα, proteases, urate crystals, and p-STAT3 have been described to induce

LMP in lysosome pathology (Baxter et al., 2006; Gomez-Sintes et al., 2016; Kreuzaler et al., 2011; Kroemer and Jaattela, 2005; Reinhardt and Lippolis, 2009). MPP^+ could inhibits complex I of the mitochondrial ETC, which results in excessive ROS production (Kotake and Ohta, 2003). MPP^+ induces glucose starvation which also increases the level of ROS(Sakamoto et al., 2017). MPTP exhibits a defective of lysosomal-mediated autophagosomal clearance due to lysosomal depletion in PD (Dehay et al., 2010). Therefore, maintaining lysosomal membrane integrity is essential for cellular protein quality control and prevention of leakage of intralysosomal components, such as lysosomal cathepsins (Papadopoulos and Meyer, 2017). Since the chemical structure of P188 is similar to plasmalemma, its insertion into membrane fascilitates restoration of membrane integrity (Tamm, 1991). P188 dramatically reduced cathepsins leakage (Fig. 2A and B, Fig. 4, A). Released from the lysosomes into the cytoplasm, cathepsins trigger caspase-dependent apoptotic cell death or release of proapoptotic factors from the mitochondria (Chwieralski et al., 2006). Activated cathepsins induces the proteolysis of Bid into tBid that facilitates mitochondrial membrane depolarization, ROS generation, cytochrome c release and caspase-3 activation. Cathepsins inhibitors reduced caspase-3 activation and cell apoptosis in MPP^+-treated cells indicating lysosomal malfunction as the upstream of apoptotic cell death pathway. P188 reduced LMP-mediated cell apoptosis *in vitro* and *in vivo* (Fig. 2C and D, Fig. 4, B). In acute or sub-acute MPTP mice models, DA neurons die quickly, so that inclusion bodies are not found in the remaining DA neurons (Meredith and Rademacher, 2011). P188 ameliorated α-synuclein accumulation, which might be due to LMP-mediated autophagosome degradation impairment in chronic MPTP mouse model. α-synuclein aggregation in cell bodies is linked to the neurodegenerative process and contributes to the behavioral deficits. P188 administration rescued behavioral impairment in chronic MPTP mouse model (Fig. 5, A-E).

The present work was aimed at addressing the issue of environmental oxidative toxin MPTP-induced DA neurons degeneration and death in PD. A compound named P188, as a biocompatible polymer consisting of two hydrophilic side-chains attached to a hydrophobic center core, offered neuroprotection against DA neuron damage and decreased protein level of aggregate-prone α-synuclein. These results demonstrate that membrane disruption significantly contributes to autophagic flux impairment and DA neuron damage, and confirm that the P188-mediated lysosomal membrane integrity restoration represents a potential therapeutic intervention for PD and related neurodegenerative diseases.

Conflicts of interest

The authors have no conflicts of interest to declare.

Acknowledgements

This study was supported by funds from the Natural Science Foundation of China (No. 31300893); the Jiangsu Province's Key Provincial Young Talents Program (No. QNRC2016261); the Research Program of Suzhou (No. SYS2018095).

References

Alcalay, R.N., Levy, O.A., Waters, C.C., Fahn, S., Ford, B., Kuo, S.H., Mazzoni, P., Pauciulo, M.W., Nichols, W.C., Gan-Or, Z., Rouleau, G.A., Chung, W.K., Wolf, P., Oliva, P., Keutzer, J., Marder, K., Zhang, X., 2015. Glucocerebrosidase activity in Parkinson's disease with and without GBA mutations. Brain 138, 2648–2658.

Baxter, F.O., Came, P.J., Abell, K., Kedjouar, B., Huth, M., Rajewsky, K., Pasparakis, M., Watson, C.J., 2006. IKKbeta/2 induces TWEAK and apoptosis in mammary epithelial cells. Development 133, 3485–3494.

Burchell, V.S., Nelson, D.E., Sanchez-Martinez, A., Delgado-Camprubi, M., Ivatt, R.M., Pogson, J.H., Randle, S.J., Wray, S., Lewis, P.A., Houlden, H., Abramov, A.Y., Hardy, J., Wood, N.W., Whitworth, A.J., Laman, H., Plun-Favreau, H., 2013. The Parkinson's disease-linked proteins Fbxo7 and Parkin interact to mediate mitophagy. Nat. Neurosci. 16, 1257–1265.

Cadichon, S.B., Le Hoang, M., Wright, D.A., Curry, D.J., Kang, U., Frim, D.M., 2007. Neuroprotective effect of the surfactant poloxamer 188 in a model of intracranial hemorrhage in rats. J. Neurosurg. 106, 36–40.

Chu, Y., Dodiya, H., Aebischer, P., Olanow, C.W., Kordower, J.H., 2009. Alterations in lysosomal and proteasomal markers in Parkinson's disease: relationship to alpha-synuclein inclusions. Neurobiol. Dis. 35, 385–398.

Chwieralski, C.E., Welte, T., Buhling, F., 2006. Cathepsin-regulated apoptosis. Apoptosis 11, 143–149.

Dehay, B., Bove, J., Rodriguez-Muela, N., Perier, C., Recasens, A., Boya, P., Vila, M., 2010. Pathogenic lysosomal depletion in Parkinson's disease. J. Neurosci. 30, 12535–12544.

Ferguson, S.A., Law, C.D., Sarkar, S., 2015. Chronic MPTP treatment produces hyperactivity in male mice which is not alleviated by concurrent trehalose treatment. Behav. Brain Res. 292, 68–78.

Fernandez, B., Fdez, E., Gomez-Suaga, P., Gil, F., Molina-Villalba, I., Ferrer, I., Patel, S., Churchill, G.C., Hilfiker, S., 2016. Iron overload causes endolysosomal deficits modulated by NAADP-regulated 2-pore channels and RAB7A. Autophagy 12, 1487–1506.

Gomez-Sintes, R., Ledesma, M.D., Boya, P., 2016. Lysosomal cell death mechanisms in aging. Ageing Res. Rev. 32, 150–168.

Gu, J.H., Ge, J.B., Li, M., Xu, H.D., Wu, F., Qin, Z.H., 2013. Poloxamer 188 protects neurons against ischemia/reperfusion injury through preserving integrity of cell membranes and blood brain barrier. PLoS One 8 e61641.

He, Q., Koprich, J.B., Wang, Y., Yu, W.B., Xiao, B.G., Brotchie, J.M., Wang, J., 2016. Treatment with trehalose prevents behavioral and neurochemical deficits produced in an AAV alpha-synuclein rat model of Parkinson's disease. Mol. Neurobiol. 53, 2258–2268.

Jackson-Lewis, V., Przedborski, S., 2007. Protocol for the MPTP mouse model of Parkinson's disease. Nat. Protoc. 2, 141–151.

Karuppagounder, S.S., Brahmachari, S., Lee, Y., Dawson, V.L., Dawson, T.M., Ko, H.S., 2014. The c-Abl inhibitor, nilotinib, protects dopaminergic neurons in a preclinical animal model of Parkinson's disease. Sci. Rep. 4, 4874.

Klaver, A.C., Coffey, M.P., Aasly, J.O., Loeffler, D.A., 2018. CSF lamp2 concentrations are decreased in female Parkinson's disease patients with LRRK2 mutations. Brain Res. 1683, 12–16.

Kotake, Y., Ohta, S., 2003. MPP+ analogs acting on mitochondria and inducing neurodegeneration. Curr. Med. Chem. 10, 2507–2516.

Kreuzaler, P.A., Staniszewska, A.D., Li, W., Omidvar, N., Kedjouar, B., Turkson, J., Poli, V., Flavell, R.A., Clarkson, R.W., Watson, C.J., 2011. Stat3 controls lysosomal-mediated cell death in vivo. Nat. Cell Biol. 13, 303–309.

Kroemer, G., Jaattela, M., 2005. Lysosomes and autophagy in cell death control. Nat. Rev. Canc. 5, 886–897.

Lazarou, M., Sliter, D.A., Kane, L.A., Sarraf, S.A., Wang, C., Burman, J.L., Sideris, D.P., Fogel, A.I., Youle, R.J., 2015. The ubiquitin kinase PINK1 recruits autophagy receptors to induce mitophagy. Nature 524, 309–314.

Lee, H.J., Yoon, Y.S., Lee, S.J., 2018. Mechanism of neuroprotection by trehalose: controversy surrounding autophagy induction. Cell Death Dis. 9, 712.

Luo, C.L., Chen, X.P., Li, L.L., Li, Q.Q., Li, B.X., Xue, A.M., Xu, H.F., Dai, D.K., Shen, Y.W., Tao, L.Y., Zhao, Z.Q., 2013. Poloxamer 188 attenuates in vitro traumatic brain injury-induced mitochondrial and lysosomal membrane permeabilization damage in cultured primary neurons. J. Neurotrauma 30, 597–607.

Luzio, J.P., Pryor, P.R., Bright, N.A., 2007. Lysosomes: fusion and function. Nat. Rev. Mol. Cell Biol. 8, 622–632.

Meredith, G.E., Rademacher, D.J., 2011. MPTP mouse models of Parkinson's disease: an update. J. Parkinson's Dis. 1, 19–33.

Meredith, G.E., Totterdell, S., Petroske, E., Santa Cruz, K., Callison Jr., R.C., Lau, Y.S., 2002. Lysosomal malfunction accompanies alpha-synuclein aggregation in a progressive mouse model of Parkinson's disease. Brain Res. 956, 156–165.

Miyara, M., Kotake, Y., Tokunaga, W., Sanoh, S., Ohta, S., 2016. Mild MPP(+) exposure impairs autophagic degradation through a novel lysosomal acidity-independent mechanism. J. Neurochem. 139, 294–308.

Papadopoulos, C., Kirchner, P., Bug, M., Grum, D., Koerver, L., Schulze, N., Poehler, R., Dressler, A., Fengler, S., Arhzaouy, K., Lux, V., Ehrmann, M., Weihl, C.C., Meyer, H., 2017. VCP/p97 cooperates with YOD1, UBXD1 and PLAA to drive clearance of ruptured lysosomes by autophagy. EMBO J. 36, 135–150.

Papadopoulos, C., Meyer, H., 2017. Detection and clearance of damaged lysosomes by the endo-lysosomal damage response and lysophagy. Curr. Biol. 27, R1330–R1341.

Pujols, J., Pena-Diaz, S., Lazaro, D.F., Peccati, F., Pinheiro, F., Gonzalez, D., Carija, A., Navarro, S., Conde-Gimenez, M., Garcia, J., Guardiola, S., Giralt, E., Salvatella, X., Sancho, J., Sodupe, M., Outeiro, T.F., Dalfo, E., Ventura, S., 2018. Small molecule inhibits alpha-synuclein aggregation, disrupts amyloid fibrils, and prevents degeneration of dopaminergic neurons. Proc. Natl. Acad. Sci. U. S. A. 115, 10481–10486.

Quinn, M., Mukhida, K., Sadi, D., Hong, M., Mendez, I., 2008. Adjunctive use of the nonionic surfactant Poloxamer 188 improves fetal dopaminergic cell survival and reinnervation in a neural transplantation strategy for Parkinson's disease. Eur. J. Neurosci. 27, 43–52.

Radulovic, M., Schink, K.O., Wenzel, E.M., Nahse, V., Bongiovanni, A., Lafont, F., Stenmark, H., 2018. ESCRT-mediated lysosome repair precedes lysophagy and promotes cell survival. EMBO J. 37.

Ravi, P.R., Aditya, N., Patil, S., Cherian, L., 2015. Nasal in-situ gels for delivery of rasagiline mesylate: improvement in bioavailability and brain localization. Drug Deliv. 22, 903–910.

Reinhardt, T.A., Lippolis, J.D., 2009. Mammary gland involution is associated with rapid down regulation of major mammary Ca2+-ATPases. Biochem. Biophys. Res. Commun. 378, 99–102.

Rukmangathen, R., Yallamalli, I.M., Yalavarthi, P.R., 2018. Biopharmaceutical potential

of selegiline loaded chitosan nanoparticles in the management of Parkinson's disease. Curr. Drug Discov. Technol. https://doi.org/10.2174/1570163815666180418144019. [Epub ahead of print].

Rusmini, P., Cortese, K., Crippa, V., Cristofani, R., Cicardi, M.E., Ferrari, V., Vezzoli, G., Tedesco, B., Meroni, M., Messi, E., Piccolella, M., Galbiati, M., Garre, M., Morelli, E., Vaccari, T., Poletti, A., 2018. Trehalose induces autophagy via lysosomal-mediated TFEB activation in models of motoneuron degeneration. Autophagy 1–21.

Sakamoto, S., Miyara, M., Sanoh, S., Ohta, S., Kotake, Y., 2017. Mild MPP(+) exposure-induced glucose starvation enhances autophagosome synthesis and impairs its degradation. Sci. Rep. 7, 46668.

Singh-Joy, S.D., McLain, V.C., 2008. Safety assessment of poloxamers 101, 105, 108, 122, 123, 124, 181, 182, 183, 184, 185, 188, 212, 215, 217, 231, 234, 235, 237, 238, 282, 284, 288, 331, 333, 334, 335, 338, 401, 402, 403, and 407, poloxamer 105 benzoate, and poloxamer 182 dibenzoate as used in cosmetics. Int. J. Toxicol. 27 (Suppl. 2), 93–128.

Tamm, L.K., 1991. Membrane insertion and lateral mobility of synthetic amphiphilic signal peptides in lipid model membranes. Biochim. Biophys. Acta 1071, 123–148.

Tanji, K., Miki, Y., Maruyama, A., Mimura, J., Matsumiya, T., Mori, F., Imaizumi, T., Itoh, K., Wakabayashi, K., 2015. Trehalose intake induces chaperone molecules along with autophagy in a mouse model of Lewy body disease. Biochem. Biophys. Res. Commun. 465, 746–752.

Tanji, K., Mori, F., Kakita, A., Takahashi, H., Wakabayashi, K., 2011. Alteration of autophagosomal proteins (LC3, GABARAP and GATE-16) in Lewy body disease. Neurobiol. Dis. 43, 690–697.

Tatton, N.A., Kish, S.J., 1997. In situ detection of apoptotic nuclei in the substantia nigra compacta of 1-methyl-4-phenyl-1,2,3,6-tetrahydropyridine-treated mice using terminal deoxynucleotidyl transferase labelling and acridine orange staining. Neuroscience 77, 1037–1048.

Wan, W., Jin, L., Wang, Z., Wang, L., Fei, G., Ye, F., Pan, X., Wang, C., Zhong, C., 2017. Iron deposition leads to neuronal alpha-synuclein pathology by inducing autophagy dysfunction. Front. Neurol. 8, 1.

Wang, R., Tan, J., Chen, T., Han, H., Tian, R., Tan, Y., Wu, Y., Cui, J., Chen, F., Li, J., Lv, L., Guan, X., Shang, S., Lu, J., Zhang, Z., 2018. ATP13A2 facilitates HDAC6 recruitment to lysosome to promote autophagosome-lysosome fusion. J. Cell Biol. 218, 267–284.

Wu, F., Xu, H.D., Guan, J.J., Hou, Y.S., Gu, J.H., Zhen, X.C., Qin, Z.H., 2015. Rotenone impairs autophagic flux and lysosomal functions in Parkinson's disease. Neuroscience 284, 900–911.

Yildirim, T., Eylen, A., Lule, S., Erdener, S.E., Vural, A., Karatas, H., Ozveren, M.F., Dalkara, T., Gursoy-Ozdemir, Y., 2015. Poloxamer-188 and citicoline provide neuronal membrane integrity and protect membrane stability in cortical spreading depression. Int. J. Neurosci. 125, 941–946.

Yoon, Y.S., Cho, E.D., Jung Ahn, W., Won Lee, K., Lee, S.J., Lee, H.J., 2017. Is trehalose an autophagic inducer? Unraveling the roles of non-reducing disaccharides on autophagic flux and alpha-synuclein aggregation. Cell Death Dis. 8 e3091.

Zatloukal, K., Stumptner, C., Fuchsbichler, A., Heid, H., Schnoelzer, M., Kenner, L., Kleinert, R., Prinz, M., Aguzzi, A., Denk, H., 2002. p62 Is a common component of cytoplasmic inclusions in protein aggregation diseases. Am. J. Pathol. 160, 255–263.